

Coccolithophore estimates of paleotemperature and paleoproductivity changes in the southeast Pacific over the past ~27 kyr

M. Saavedra-Pellitero,¹ J. A. Flores,¹ F. Lamy,² F. J. Sierro,¹ and A. Cortina¹

Received 8 July 2009; revised 19 October 2010; accepted 2 November 2010; published 27 January 2011.

[1] We provide high-resolution sea surface temperature (SST) and paleoproductivity data focusing on Termination 1. We describe a new method for estimating SSTs based on multivariate statistical analyses performed on modern coccolithophore census data, and we present the first downcore reconstructions derived from coccolithophore assemblages at Ocean Drilling Project (ODP) Site 1233 located offshore Chile. We compare our coccolithophore SST record to alkenone-based SSTs as well as SST reconstructions based on dinoflagellates and radiolaria. All reconstructions generally show a remarkable concordance. As in the alkenone SST record, the Last Glacial Maximum (LGM, 19–23 kyr B.P.) is not clearly defined in our SST reconstruction. After the onset of deglaciation, three major warming steps are recorded: from 18.6 to 18 kyr B.P. (~2.6°C), from 15.7 to 15.3 kyr B.P. (~2.5°C), and from 13 to 11.4 kyr B.P. (~3.4°C). Consistent with the other records from Site 1233 and Antarctic ice core records, we observed a clear Holocene Climatic Optimum (HCO) from ~8–12 kyr B.P. Combining the SST reconstruction with coccolith absolute abundances and accumulation rates, we show that colder temperatures during the LGM are linked to higher coccolithophore productivity offshore Chile and warmer SSTs during the HCO to lower coccolithophore productivity, with indications of weak coastal upwelling. We interpret our data in terms of latitudinal displacements of the Southern Westerlies and the northern margin of the Antarctic Circumpolar Current system over the deglaciation and the Holocene.

Citation: Saavedra-Pellitero, M., J. A. Flores, F. Lamy, F. J. Sierro, and A. Cortina (2011), Coccolithophore estimates of paleotemperature and paleoproductivity changes in the southeast Pacific over the past ~27 kyr, *Paleoceanography*, 26, PA1201, doi:10.1029/2009PA001824.

1. Introduction

[2] The Pacific Ocean plays an important role in modulating global climate at seasonal, interannual (El Niño–Southern Oscillation, ENSO), millennial and orbital time scales [Cane, 1998; Clement *et al.*, 1999]. The ENSO cycle of alternating El Niño and La Niña events is a good example of instabilities originated in the tropical Pacific through interactions between the ocean and the atmosphere, which ultimately modify hydrographic conditions and alter the climate at a global scale [Cane, 1998; McPhaden *et al.*, 2006]. However, little is known about past changes in SST and related paleoceanographic conditions in the Southeast (SE) Pacific. Various paleotemperature proxies were used, including faunal-based transfer functions (e.g., planktonic foraminifera), alkenones and Mg/Ca ratios in foraminiferal shells [e.g., Wefer *et al.*, 1999; Lea, 2003; Kucera *et al.*, 2005a]. Nevertheless, significant discrepancies have been observed when a SST multiapproach has been performed on the same marine sediment cores [e.g., Chapman *et al.*, 1996;

Mix, 2006; Koutavas and Sachs, 2008; Steinke *et al.*, 2008; Leduc *et al.*, 2010]. Here, we compare alkenone SSTs with the SST estimations derived from a new method proposed in this paper (transfer function-like) using coccolithophore assemblages in a marine sedimentary sequence off southern Chile.

[3] It has been reported that transfer functions based on diatom and radiolarian species offer a reliable tool for estimating paleoceanographic changes in the SE Pacific [Pisias *et al.*, 1997, 2006; Abrantes *et al.*, 2007], together with planktonic foraminifera [Mix *et al.*, 1999; Feldberg and Mix, 2002; Kucera *et al.*, 2005b; Morey *et al.*, 2005]. However, no transfer function using coccolithophores has been done for the SE Pacific. Coccolithophores are a group that includes all haptophyte algae with highly characteristic calcified scales called coccoliths at some stage of their life cycle [Pienaar, 1994; Billard and Inouye, 2004]. This carbonate-producing algae group thrives under a broad spectrum of oceanic regimes. They predominate in the photic zones of stratified waters from the subtropical and tropical regions of the world [Brand, 1994], but they are also significant contributors to the total phytoplankton community in coastal upwelling domains [Mitchell-Innes and Winter, 1987; Giraudeau *et al.*, 2000; Boeckel and Baumann, 2004].

[4] The new methodology proposed consists of a multivariate statistical analysis performed on modern census coccolithophore data from surface sediments covering the

¹Department of Geology, University of Salamanca, Salamanca, Spain.

²Alfred Wegener Institute for Polar and Marine Research, Bremerhaven, Germany.

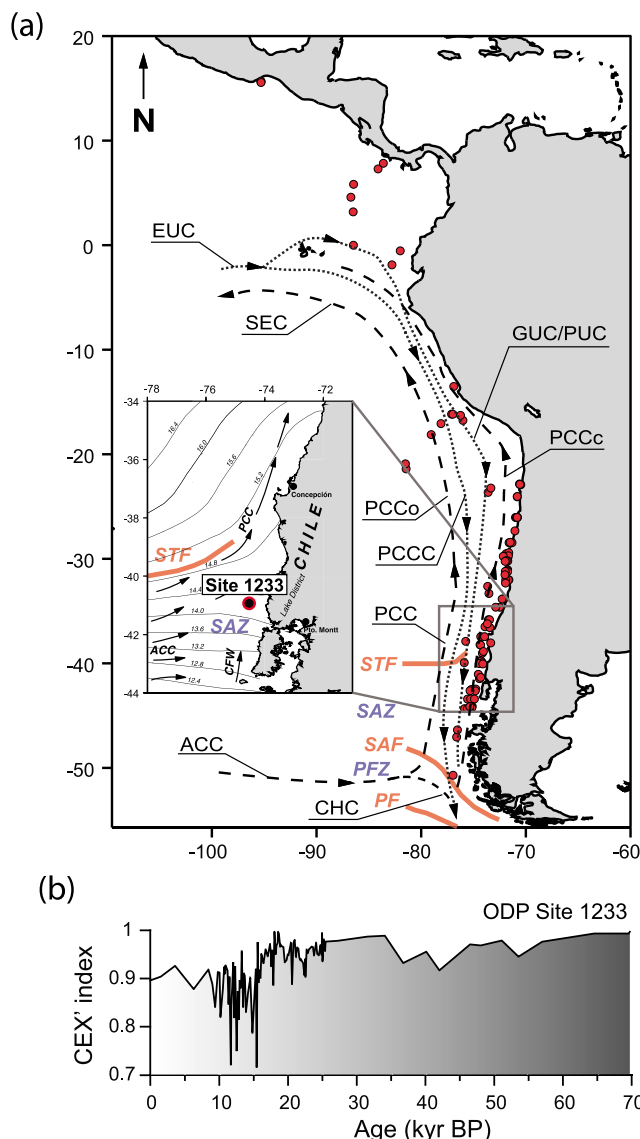


Figure 1. (a) Major surface and subsurface oceanic circulation patterns in the study area (modified from *Feldberg and Mix* [2002], *Strub et al.* [1998], and *Lamy et al.* [2004]). Surface currents (black dashed lines): Antarctic Circumpolar Current (ACC), Chilean Fjord Water (CFW), Cape Horn Current (CHC), Peru-Chile Current (PCC), Peru-Chile Coastal Current (PCCc), Peru-Chile Oceanic Current (PCCo), and South Equatorial Current (SEC). The subsurface currents (dotted lines) are the Peru-Chile Countercurrent (PCCC), the Peru Undercurrent (PUC), and the Equatorial Undercurrent (EUC). Oceanic fronts marked and areas between are as follows: Subtropical Front (STF), Subantarctic Zone (SAZ), Subantarctic Front (SAF), Polar Front Zone (PFZ), and Polar Front (PF) [*Orsi et al.*, 1995]. The inset shows the location of the ODP Site 1233. Annual mean sea surface temperatures are in °C. (b) CEX' index calculated for ODP Site 1233.

equatorial and SE Pacific area affected by different environmental factors [*Saavedra-Pellitero et al.*, 2010] and their application to Ocean Drilling Project (ODP) Site 1233 well-dated sediments [*Lamy and Kaiser*, 2009] to reconstruct past SSTs offshore Chile during the past ~27 kyr with high temporal resolution. Similar results to those of independent alkenone-based SST reconstructions from the same site were obtained, suggesting that our coccolith-based reconstruction is a reliable tool, at least in the realm of the SE Pacific.

2. Oceanographic and Atmospheric Setting of the Southeastern Pacific Ocean

[5] The oceanographic features of the study area are described in detail by *Strub et al.* [1998] and *Shaffer et al.* [1995]. The large-scale circulation is revealed by fields of surface temperature and salinity [*Strub et al.*, 1998]. The circulation pattern is dominated by the equatorward flowing Peru-Chile Current (PCC), starting between 40 and 45°S, where the Antarctic Circumpolar Current (ACC) approaches the South American continent (Figure 1a). The steepest SST gradient within the ACC is strongly related to the main atmospheric circulation member of the Southern Hemisphere (SH), i.e., the westerly wind belt [*Streten and Zillmann*, 1984]. The ACC splits at ~43°S into the northward flowing PCC and the southward flowing Cape Horn Current (CHC) [*Strub et al.*, 1998]. The PCC flows northward along the western South American coast before it turns westward close to the equator to form the South Equatorial Current (SEC). Beneath the SEC lies the Equatorial Undercurrent (EUC), which flows eastward. Both the EUC and the SEC contribute to the equatorial cold tongue that extends westward to 10°W longitude [*Wyrtki*, 1981] (Figure 1a). The offshore Ekman flow drives a perennial upwelling of cool, nutrient-rich waters, resulting in one of the biologically most productive regions of the world's oceans [*Berger et al.*, 1987].

[6] South of ~38°S, the year-round onshore blowing winds (the Southern Westerlies, SW) generally prevent coastal upwelling [*Miller*, 1976; *Strub et al.*, 1998; *Kim et al.*, 2002]. The SW and associated storm tracks bring heavy rainfall, resulting in large fresh water fluxes to the coastal ocean, and they are the origin of the low-salinity tongue spreading northward along the southern and central Chilean margin [*Dávila et al.*, 2002]. The increasing influence of storm tracks southward offshore Chile together with the steep Chilean topography result in a huge input of terrigenous material and a clear dominance of terrigenous sediments along the Chilean continental slope [*Lamy et al.*, 1998]. In these coastal southern areas, the availability of iron increases strongly due to high river discharge, which results in a very high productivity [e.g., *Iriarte et al.*, 2007] that is even more pronounced than in the upwelling-dominated parts offshore central and northern Chile [*Hebbeln et al.*, 2000].

[7] The study area is also characterized by a sequence of oceanic fronts (Figure 1a). The northern boundary of the ACC is limited by the Subtropical Front (STF) [*Orsi et al.*, 1995]. The zone between the STF and the SAF (Subantarctic Front) is referred to as the SAZ (Subantarctic Zone)

[Orsi *et al.*, 1995], and the PF marks the location where the Antarctic Surface Water moving northward sinks below the Subantarctic Water [Deacon, 1933].

3. Material and Methods

3.1. Surface Sediment Samples

[8] As the basis for the analysis, coccolith census counts from equatorial and SE Pacific core tops (15.71°N–50.65°S and 70.49°W–95.29°W) [Saavedra-Pellitero *et al.*, 2010] were used (Figure 1a). The surface sediment data set consists of 96 surface sediment samples with a generally good degree of preservation, mostly located above the present Carbonate Compensation Depth (CCD) and the Carbonate Lysocline in the area (CL). Depths vary depending on the location; e.g., CL = ~3500 m and CCD = ~4100 m in the southern Pacific [Broecker and Broecker, 1974; Berger *et al.*, 1976] and CL = 3800–4000 m in the equatorial Pacific [Thompson, 1976; Farrell and Prell, 1989]. For the coccolith analysis, the uppermost undisturbed centimeter was selected, assuming that surface sediment samples mostly represent present-day conditions. Mean annual values of the different physical, chemical and biological parameters variables were chosen in order to characterize the water conditions of the living coccolithophores corresponding to each station [Saavedra-Pellitero *et al.*, 2010]: SST in °C, sea surface salinity (SSS in psu), nitrate (in $\mu\text{mol/l}$), phosphate (in $\mu\text{mol/l}$), silicate (in $\mu\text{mol/l}$) and chlorophyll concentrations (in $\mu\text{g/l}$).

3.2. Fossil Data Set: ODP Site 1233

[9] ODP Site 1233 is located off southern Chile (41°00'S, 74°27'W) at a water depth of 838 m, 38 km offshore (20 km off the continental shelf) in a small fore-arc basin on the upper continental slope. The sediments at this site are dominated by terrigenous components (clay and silty clay), with varying, but generally low, amounts of calcareous components; primarily calcareous nannofossils and foraminifera [Mix *et al.*, 2003]. This site is located outside the pathways of major turbidity currents [Mix *et al.*, 2003] and shows a continuous and undisturbed sedimentary record. Furthermore, the subantarctic site is under the influence of the Southern Westerlies at the northern margin of the ACC, and the surrounding area is affected by a prominent low-salinity tongue originated from freshwater input in the Chilean fjord region [Lamy *et al.*, 2004]. In the past, mean sedimentation rates at Site 1233 were extremely high (~100 cm/kyr in the Holocene and even were higher during the last glacial [Lamy *et al.*, 2001; Kaiser *et al.*, 2005]), offering the possibility of studying climate and ocean variability at submillennial to millennial time scales [e.g., Kaiser *et al.*, 2007].

[10] Five Advanced Piston Corer holes were drilled at Site 1233 to ensure a complete stratigraphic overlap between cores from different holes, and a composite section was constructed representing 135.65 mcd (meters of composite depth) [Mix *et al.*, 2003]. The age model for the sedimentary sequence of site 1233 has been published previously by Lamy *et al.* [2004] and has been updated by Kaiser *et al.* [2005] and Lamy *et al.* [2007].

[11] Ninety-three samples for the interval, ranging from ~27 kyr B.P. to 10 kyr B.P., were chosen to record millennial-scale changes, mainly during the last deglaciation (also named Termination 1, with a temporal resolution of ~160 years on average, see the auxiliary material).¹ Additionally, 21 samples were added as control points for younger than 10 kyr B.P. and the older part of the Site 1233 record back to ~70 kyr.

3.3. Techniques for the Preparation and Identification of Taxa

[12] For this study, we followed the Backman and Shackleton [1983] and Flores and Sierro [1997] techniques, which allowed us to obtain quantitative results: relative and absolute abundances (% and coccoliths/g of sediment) together with fluxes (nannofossil accumulation rate, NAR, coccoliths $\text{cm}^{-2} \text{kyr}^{-1}$). The formula used to calculate fluxes followed Flores and Sierro [1997]: $\text{NAR} = [(n R^2 V^2)/(r^2 g v)] d S$, where n is the number of nannofossils counted in a random light microscope scanned area; R is the radius of the Petri dish used; V is the volume of the water added to the dry sediment; r is the radius of the visual field used in the counting; g is the dry sediment weight; v is the volume of mixture withdrawn with the micropipette; d is the estimated dry density of the sediment, and S is the linear sedimentation rate. The NAR has been used as a reference for high paleo-productivity of coccolithophores and particle flux out of the mixed layer [e.g., Steinmetz, 1994; Baumann *et al.*, 2004; López-Otálvaro *et al.*, 2009].

[13] Coccolith identification was carried out using a Leica DMRXE® and a Nikon Eclipse 80i® polarized microscopes at magnifications of 1000X and 1250X. All slides were analyzed with a uniform counting procedure, and a minimum of 400 coccoliths were counted per sample to ensure minimum error [Fatela and Taborda, 2002]. The 14 most common taxa or groups of coccoliths considered in this study were: *Calciosolenia* sp., *Calcidiscus leptoporus*, *Coccolithus pelagicus*, *Emiliania huxleyi*, *Florisphaera profunda*, *Gephyrocapsa muelleriae*, *Gephyrocapsa oceanica*, *Helicosphaera carteri*, *Rhabdosphaera clavigera*, “small” *Gephyrocapsa* (that include *Gephyrocapsa* < 3 μm), *Syracosphaera* spp., *Umbellosphaera* spp., *Umbilicosphaera* spp. and *Oolithotus* sp. Some taxa appeared infrequently (i.e., the nannolith *Braarudosphaera bigelowii* at ODP Site 1233) and were excluded from the statistical treatment. Our analysis included these 14 groups, accounting for 100%.

3.4. Species Diversity and CEX' Index

[14] We calculated the Shannon index (H') using the Palaeontological Statistics (PAST™) software with the following equation for the fossil samples:

$$H' = - \sum_{i=1}^S \frac{n_i}{N} \ln \frac{n_i}{N},$$

where n_i is the number of individuals in species i ; S is the number of taxa, and N is the total number of all individuals.

¹Auxiliary material data sets are available at <ftp://ftp.agu.org/apend/pa/2009pa001824>. Other auxiliary material files are in the HTML.

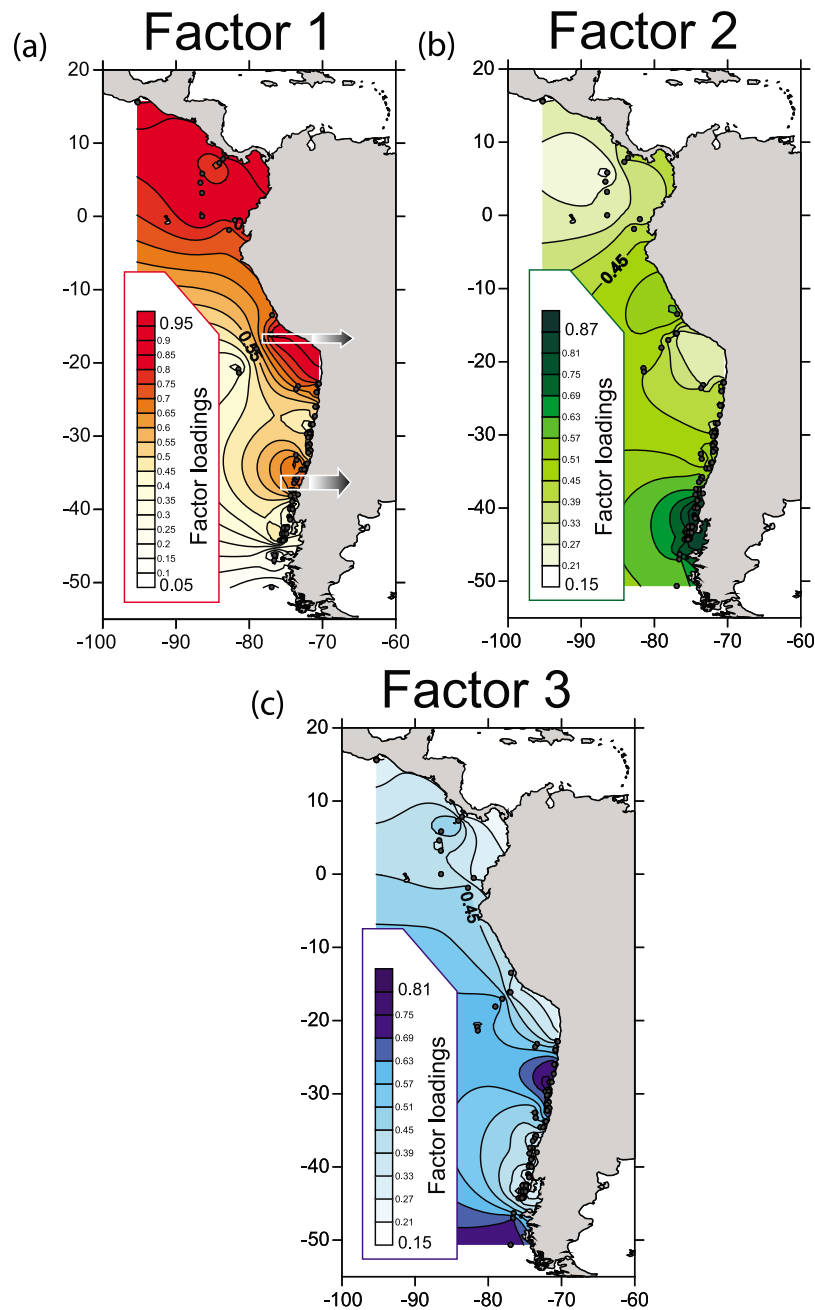


Figure 2. Contour map of the factor loadings for (a) factor 1, (b) factor 2, and (c) factor 3 in the stations that configure the present-day data set. Main dissolution intervals defined by LM observations have been marked with arrows [Saavedra-Pellitero *et al.*, 2010].

H' varies from 0 for communities with only a single taxon to high values for communities with many taxa, each with few individuals. High abundances and diversity values have been recorded in the Pacific Subtropical Front (STF, Figure 1a) and Subantarctic Front (SAF) [Findlay *et al.*, 2005], but a general decrease takes place toward the South [Winter *et al.*, 1994] until monospecific assemblages of *E. huxleyi* occur south of the Polar Front (PF) [Gravalosa *et al.*, 2008]. Thus, a higher species diversity index can be related to higher SSTs.

[15] We also calculated a modification of the CEX' index [Dittert *et al.*, 1999; Boeckel and Baumann, 2004], which was classically used to estimate the effect of carbonate dissolution on the coccolith assemblages: $CEX' = (\% E. huxleyi + \% \text{“small” } Gephyrocapsa) / (\% E. huxleyi + \% \text{“small” } Gephyrocapsa + \% C. leptoporus)$. This index was initially based on the differential dissolution of the small and delicate placoliths of *E. huxleyi* and “small” *Gephyrocapsa* and the strongly calcified coccoliths of *Calcidiscus leptoporus* assuming certain constancy in the

Table 1. Factor Scores Obtained in the PCA Factor Analysis Performed in the Present-Day Data Set (Surface Sediment Samples)^a

	Factor 1 (Present)	Factor 2 (Present)	Factor 3 (Present)
<i>F. profunda</i>	2.12	-0.54	0.32
<i>C. leptoporus</i>	-0.46	0.15	1.93
<i>H. carteri</i>	-1.15	-0.85	2.03
<i>G. oceanica</i>	2.17	-0.35	-0.23
<i>G. muellerae</i>	0.33	1.07	0.22
<i>Syracosphaera</i>	-0.43	-0.59	-0.62
<i>Umbilicosphaera</i>	-0.05	-1.19	0.16
<i>Umbellosphaera</i>	-0.45	-0.72	-0.67
<i>Calciosolenia</i>	-0.47	-0.70	-0.72
<i>C. pelagicus</i>	-1.00	1.23	-1.28
<i>R. clavigera</i>	-0.51	-0.72	-0.59
<i>Oolithotus</i>	-0.34	-0.18	-1.18
<i>E. huxleyi</i>	-0.16	1.59	0.30
“Small” <i>G</i>	0.40	1.82	0.32

^aRotation, varimax normalized; extraction, principal components. Bold values indicate the species which define each factor.

assemblage. Carbonate dissolution has a more important effect on small placoliths than on *C. leptoporus*, and therefore the ratio of these taxa will decrease with increasing dissolution. Nevertheless CEX' index was interpreted here in a different way. Because the coccolithophore assemblages becomes *E. huxleyi*-monospecific southward [e.g., McIntyre and Bé, 1967; Winter et al., 1994], rapid excursions of the CEX' during deglaciation can be linked to rapid shifts in the environmental conditions that influenced the ecological preferences of coccolithophores. Increases in CEX' values downcore would be related to a prominent *E. huxleyi* monospecific flora and to an equatorward displacement of hydrological fronts, and decreases in the index to a poleward shift of whole system (Figure 1b).

3.5. Statistics

[16] Our method, based on multivariate statistical analyses performed with the Statistica 7.0™ software package is explained in detail in the auxiliary material. Factor analysis techniques are generally used to reduce the number of variables and to detect structures in the relationships among variables (i.e., to classify variables). In this study, the variables were highly correlated, such that grouping stations into factors allowed us to know how many statistically independent artificial end-members there were in the equatorial and SE Pacific and to analyze their distribution patterns together with the taxa dominant in each of them.

[17] The statistical procedure proposed allowed us to detect one factor linked to SST and to calculate SSTs for the past ~27 ky B.P. The SSTs estimated were compared with those derived from alkenones [Lamy et al., 2004, Kaiser et al., 2005; Lamy et al., 2007] in order to validate our methodological approach to the paleodata. Additionally, we compared our new SSTs estimation with other records from Site 1233 (radiolarian and pollen records [Pisias et al., 2006]) and temperature records from Antarctic ice cores such as the Byrd ice core [Blunier and

Table 2. Correlation Matrix Obtained Between the Factors From the Present Data Set and the Selected Environmental Variables^a

	Factor 1 (Present)	Factor 2 (Present)	Factor 3 (Present)
SSS average	0.45	-0.71	0.44
SST average	0.67	-0.73	0.01
Nitrate average	0.32	-0.02	-0.37
Phosphate average	0.53	-0.16	-0.41
Silicate average	0.73	-0.50	-0.24
Chlorophyll average	-0.05	0.26	-0.12

^aBold values correspond to significant correlations at $p < 0.05$.

Brook, 2001] and the EPICA Dronning Maud Land ice core [EPICA Community Members, 2006].

4. Results

4.1. Nannofloral Factors

4.1.1. Surface Sediments

[18] The Principal Component Analysis (PCA) performed on the present-day data set [Saavedra-Pellitero et al., 2010] indicated the existence of three main factors (Figure 2), characterized below.

[19] Factor 1, in which the important species are *F. profunda* and *G. oceanica* (Table 1) and which explains 31.58% of the total variance, dominates from 15°N to 25°S and from ~33° to 38°S (Figure 2a), this latter area being interpreted as one of carbonate dissolution. Saavedra-Pellitero et al. [2010] reported that this factor is highly correlated with the silicate content (0.73) and SST (0.67), and, to a lesser extent, with phosphate (0.53) and SSS (0.45 (Table 2)). Owing to the low factor 1 loadings at 41°S, in order to reconstruct SSTs at ODP Site 1233 this factor was discarded.

[20] Factor 2, in which the important species are *E. huxleyi*, “small” *Gephyrocapsa*, *C. pelagicus* and *G. muellerae* (Table 1) and which explains 33.87% of the total variance, dominates from 38°S to 47°S offshore Chile (Figure 2b). Factor 2 is strongly anticorrelated with SST and SSS (-0.73

Table 3. Factor Scores Obtained in the PCA Factor Analysis Performed in the Past Data Set (ODP Site 1233)^a

	Factor 2 (Past)	Factor 3 (Past)	“Nonanalog” Factor (Past)
<i>F. profunda</i>	-0.24	0.48	-0.86
<i>C. leptoporus</i>	-0.36	1.64	-0.67
<i>H. carteri</i>	-1.01	1.57	-0.85
<i>G. oceanica</i>	-1.85	0.33	2.71
<i>G. muellerae</i>	1.29	0.08	1.02
<i>Syracosphaera</i>	-0.21	-0.58	-0.62
<i>Umbilicosphaera</i>	-0.64	-0.39	-0.17
<i>Umbellosphaera</i>	-0.24	-0.83	-0.39
<i>Calciosolenia</i>	-0.24	-0.88	-0.40
<i>C. pelagicus</i>	0.76	-1.61	0.17
<i>R. clavigera</i>	-0.26	-0.74	-0.47
<i>Oolithotus</i>	-0.27	-0.84	-0.38
<i>E. huxleyi</i>	1.54	1.17	-0.31
“Small” <i>G</i>	1.73	0.60	1.22

^aRotation, varimax normalized; extraction, principal components. Bold values indicate the species which define each factor.

Table 4. Correlation Matrix Between Present and Past Factors^a

	Factor 1 (Present)	Factor 2 (Present)	Factor 3 (Present)
Factor 2 (past)	-0.20	0.85	-0.09
Factor 3 (past)	0.20	0.17	0.92
“Nonanalog” factor (past)	0.54	0.36	-0.15

^aBold values correspond to significant correlations at $p < 0.05$.

and -0.71), and to a lesser extent with the silicate content (-0.50 (Table 2)). This factor is linked to fresh water fluxes to the coastal ocean and, broadly, to the above mentioned low-salinity cold tongue [Saavedra-Pellitero et al. 2010]. It is of potential use for estimating SSTs.

[21] Factor 3 explains $\sim 28\%$ of the total variance and its major contributors are *C. leptoporus* and *H. carteri* (Table 1). It dominates from 25° to 33°S (Figure 2c) in the northernmost area of the Chilean upwelling system and at two stations south of the study area owing to the proximity of the SAF, where a strong increase in *C. leptoporus* has been observed [Gravalosa et al., 2008] and where the signal is probably influenced by dissolution. Saavedra-Pellitero et al. [2010] indicated that this factor is correlated with SSS, anticorrelated with phosphate (0.44 and -0.41) and, to a lesser extent, anticorrelated with nitrate contents (-0.37 (Table 2)).

4.1.2. Sedimentary Record and Paleoenvironmental Calibration

[22] Three factors are sufficient to describe the temporal downcore variability at ODP Site 1233 (Table 3). For paleoenvironmental calibration, comparison of the three factors from the present-day database (“present”) and the three from the sedimentary record (“past”) was performed

by means of a correlation matrix made using the factor scores (Table 4). It revealed that two of the factors from the sedimentary record are equivalent to the modern factor 2 and factor 3 ($r = 0.85$ and $r = 0.92$ (Table 4 and Figure 3)), although there is a third factor that dominates during early marine isotope stage (MIS) 3 and MIS 4 (~ 46 to 70 kyr B.P.) and has no representative in present-day conditions (“non-analog”) (Figure 4a). We infer that it most likely represents fertile water conditions because the dominant species is *G. oceanica* ($< 4 \mu\text{m}$), which has classically been observed to respond to intermittent fertile waters by increasing its population size and which, under certain favorable conditions, might even reach bloom proportions [Kleijne et al., 1989; Brown and Yoder, 1994; Winter et al., 1994; Young, 1994; Giraudeau and Bailey, 1995; Broerse et al., 2000].

[23] Accordingly we can only use factors 2 and 3 for our downcore reconstructions, because they are identical to the factors found in present-day conditions and can be linked directly to environmental parameters. Factor 2 dominates in the past, explaining $\sim 43\%$ of the total variance (Table 3 and Figure 3a), with the score species “small” *Gephyrocapsa*, *E. huxleyi*, *G. muelleriae* and *C. pelagicus*. Its predominance runs from late MIS 3 to the Holocene (~ 40 kyr B.P. to the present time (Figure 4a)), except during the last deglaciation, where factor 3 stands out (specifically from ~ 18.5 to ~ 8.5 kyr B.P. (Figure 4a)), suggesting the onset of different oceanographic conditions during deglaciation. The score species for factor 3, which explains 33.37% of the variance, are *C. leptoporus* and *H. carteri* (Table 3 and Figure 3b).

4.2. SST Estimation at ODP Site 1233

[24] Alkenones, a series of long-chain (C_{37} , C_{38} , C_{39}) primarily diunsaturated and triunsaturated methyl or ethyl ketones, are produced by a specific class of phytoplankton

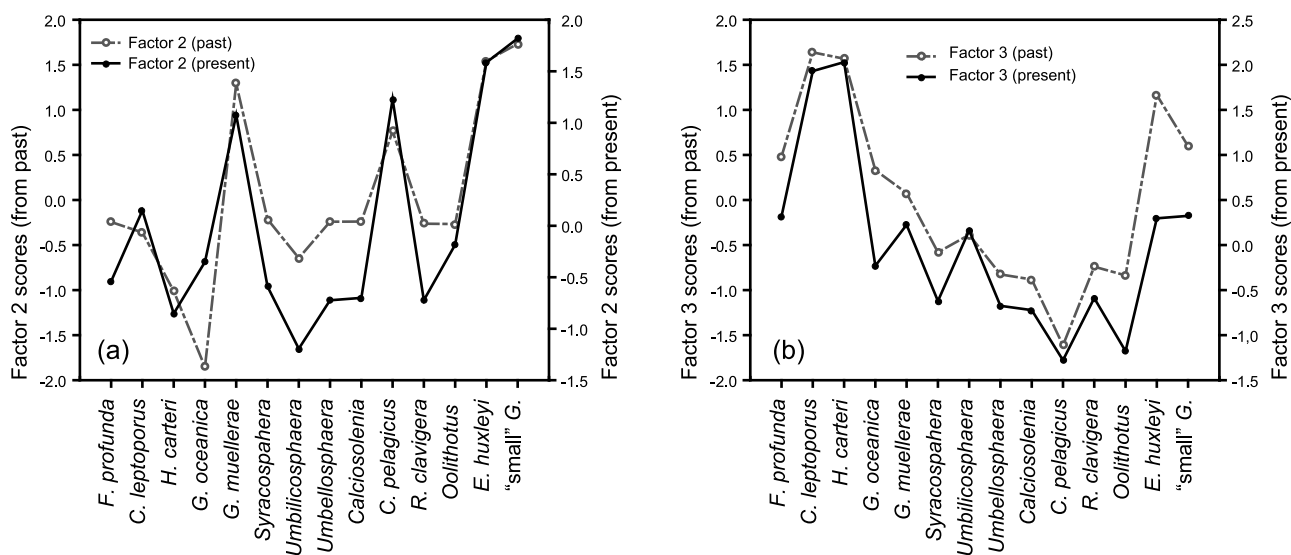


Figure 3. (a) Derived factor score graphics for factor 2 (from the present-day data set (“present”) and from the ODP Site 1233 sedimentary record (“past”). Coccolithophore taxa are given in the x axis, and factor score values are represented in the y axis. (b) Derived factor score graphics for factor 3 (from the present-day data set (“present”) and from the ODP Site 1233 sedimentary record (“past”). Coccolithophore taxa are given in the x axis, and factor score values are represented in the y axis.

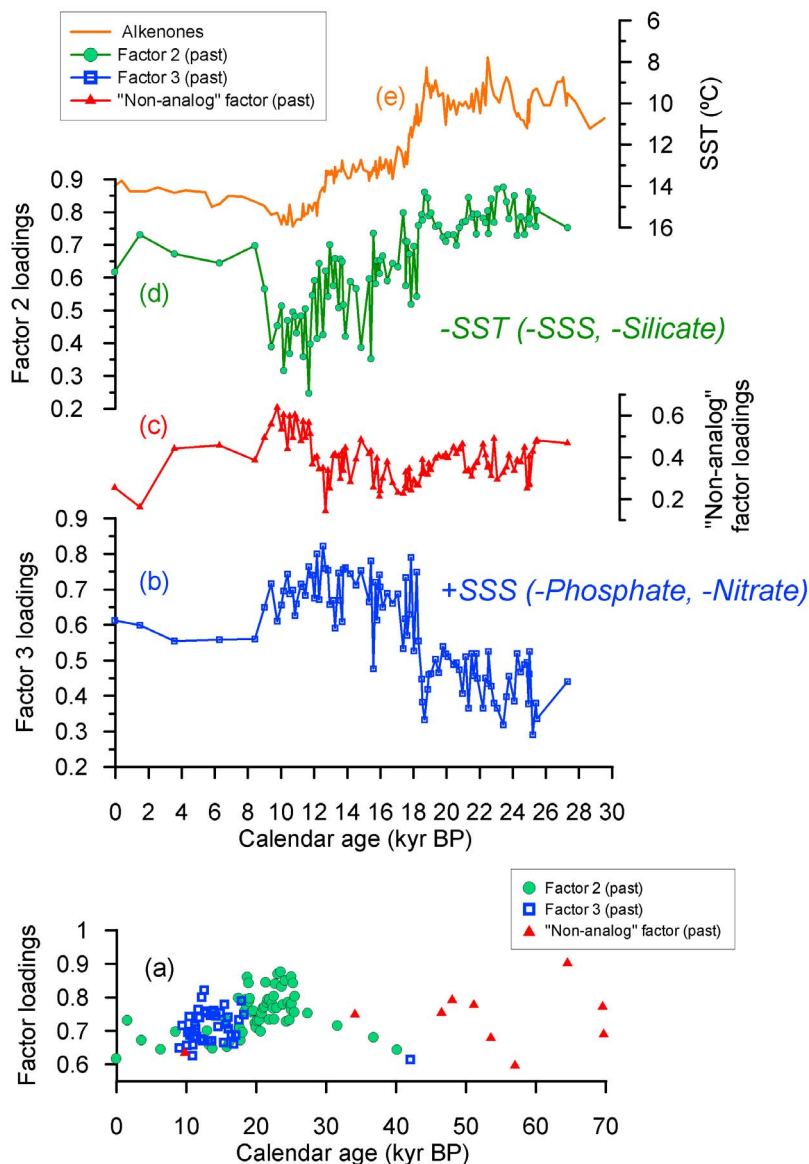


Figure 4. (a) Distribution of the dominant factors for each sampling point at ODP Site 1233 for the last ~70 kyr (sedimentary record), indicated as follows: factor 2 with circles, factor 3 with squares, and “non-analog” factor with triangles. Detail of Figure 4a showing the (b) factor 3 factor loadings for the last ~30 kyr, (c) “nonanalog” factor loadings, (d) factor 2 loadings, and (e) SST estimates derived from alkenones [Lamy et al., 2004, 2007].

broadly represented by the genus *Gephyrocapsa* [Marlowe et al., 1990] and specifically by *E. huxleyi* [Volkman et al., 1980]. Changes in environmental conditions affect the lipid composition of microscopic algae [Volkman et al., 1980] and SSTs can be estimated from the analysis of long-chain ketone compositions preserved in sediment cores [Prahl and Wakeham, 1987]. It is therefore of interest to compare SSTs derived from alkenones and SSTs obtained from the assemblages of their recognized sources: coccolithophores. In this study, a comparison of the alkenone SSTs record [Lamy et al., 2004, Kaiser et al., 2005; Lamy et al., 2007] with our data validates our procedure for reconstructing oceanographic parameters.

[25] The correlation matrix generated using factor loadings from the coccolith assemblage that characterize the three factors at Site 1233 and SST values from alkenones indicates a high coefficient of correlation ($r = 0.74$ (Table 5)) between alkenones and factor 3. It was already shown that factor 3 is slightly correlated to SSS and anticorrelated to phosphate and nitrate contents (Table 2), but not to SST. Nevertheless, a relationship can be inferred between SST and factor 3 loadings only considering the samples located off-shore Chile. This fact would explain the correlation between the ODP Site 1233 factor 3 loadings and alkenones. However, further future work would be required to disentangle this discrepancy.

Table 5. Correlation Matrix Between Past Factors and the SST Alkenones^a

	Factor 2 (Past)	Factor 3 (Past)	“Nonanalog” Factor (Past)
Alkenones	-0.6425	0.74	0.08

^aThe bold value indicates which factor was used to estimate nannofloral SSTs at ODP Site 1233.

[26] The same matrix indicates that factor 2 at Site 1233 is strongly and negatively correlated with alkenone-derived SSTs ($r = -0.64$ (Table 5)). This is consistent with our results concerning the modern factor 2 correlation with SST ($r = -0.73$ (Table 2)). These high correlation coefficients provide the necessary confidence to explore the use of this relationship for estimating paleotemperatures from fossil assemblages.

[27] To estimate SSTs, we compared the log-transformed average annual SST and factor 2 loadings and obtained a linear regression equation, with a significant correlation of $r^2 = 0.57$. The transfer function equation is $y = 1.3538 - 0.3515x$, where y is the logarithm of SST and x is the factor 2 loading (Figure 5a). To assess potential biases in the transfer function, which might yield inaccurate results, we calculated the correlation coefficient between the estimated mean annual SSTs and the observed (or measured) mean annual SSTs ($r = 0.75$ (Figure 5b)) and the temperature residuals (the difference between the estimated minus the observed SST).

[28] A comparison of temperature residuals and the measured SSTs (Figure 5c) indicates that at stations where present-day SSTs are below 11°C, the SSTs using our function are overestimated, owing to the absence of data south of 45–50°S. In contrast, the low negative values of SST residuals indicate an underestimation of SSTs at stations where factor 1 dominates (thus, factor 2 is not valid for reconstructing SST at these locations (Figure 5d)). However, SST estimations for the deglaciation performed in this study vary from 11 to 16°C, i.e., within the acceptable range.

[29] Focusing exclusively on the results obtained for the last deglaciation, a simple linear correlation between SSTs estimated by coccolithophore assemblages and alkenones for the interval from ~27 kyr B.P. to 10 kyr B.P. (Figure 6) was performed, and the resulting high coefficient ($r = 0.81$) validated our SST reconstruction for this time frame. To improve the accuracy of the results, a confidence interval at the 95% level was considered (Figure 6a).

4.3. Paleoproductivity Estimates

[30] Our coccolith-based SST results were completed with additional estimations of the number of coccoliths per gram of sediment and accumulation rates. Because productivity is much greater in eutrophic conditions, a very large proportion of total coccolith production occurs under such conditions [Baumann *et al.*, 2005]. Hence, for this study we assume that higher NAR values in the absence of dissolution correspond to higher nutrient availability and coccolithophore productivity.

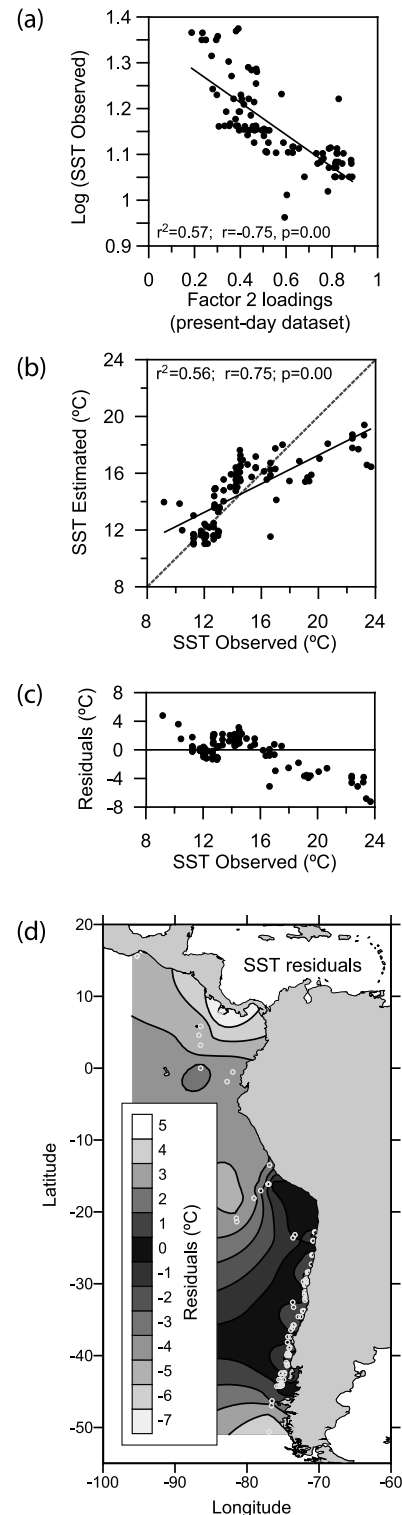


Figure 5. (a) Factor loadings from factor 2 (from the present-day data set) versus measured SSTs (in °C), (b) SSTs measured versus estimated SSTs, (c) observed SSTs versus SST residuals (estimated minus measured, in °C), and (d) SST residuals at core top locations in the equatorial and southeastern Pacific.

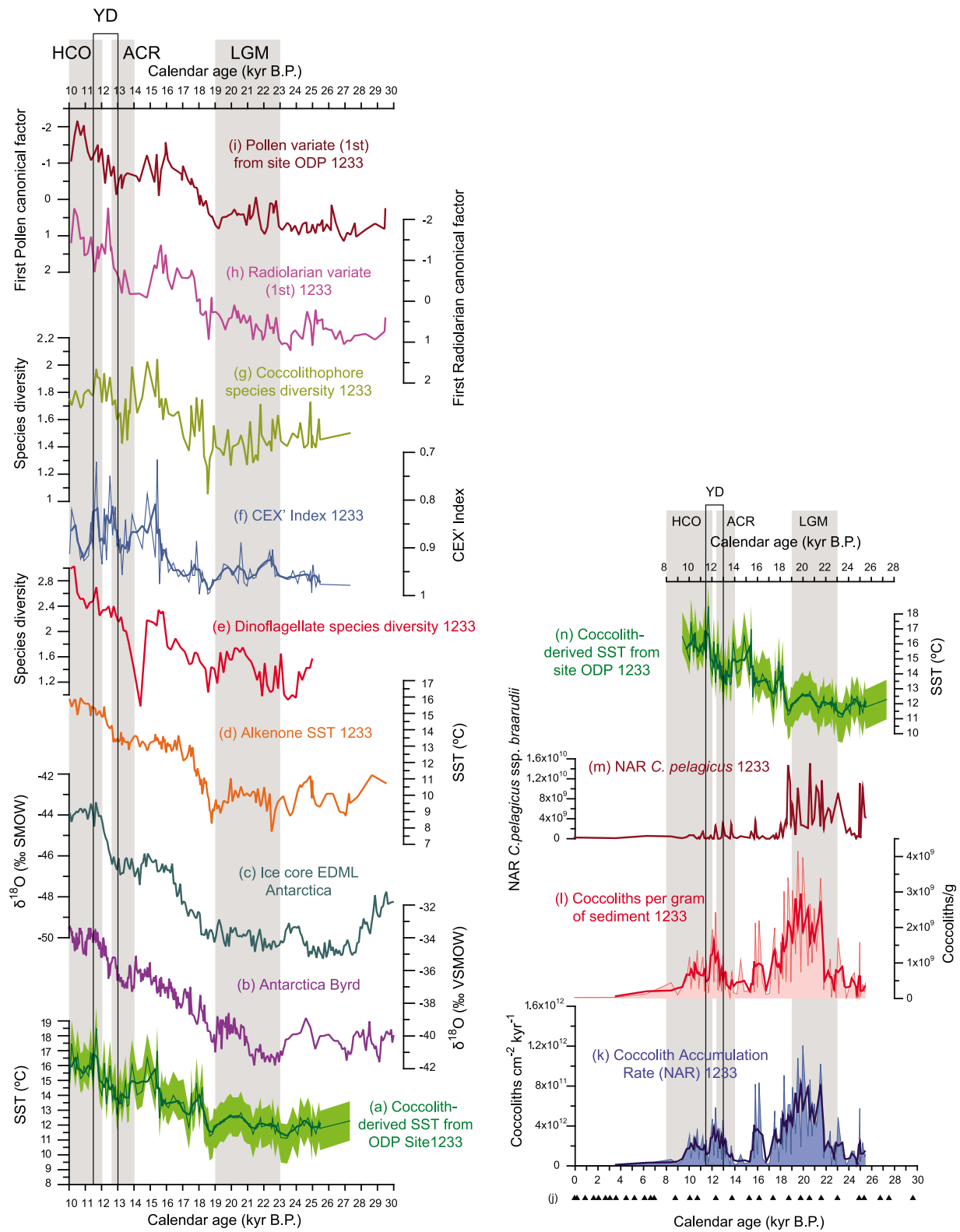


Figure 6

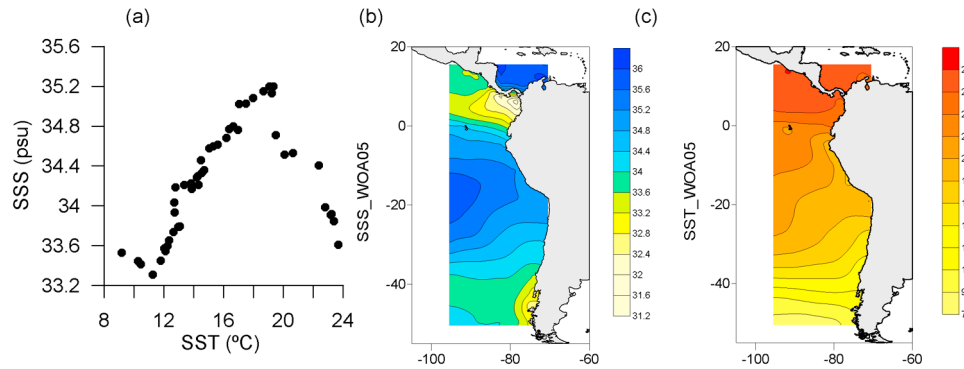


Figure 7. (a) SST (in °C) versus SSS (in psu) corresponding to the core top locations of the present-day database. (b) Mean annual sea surface salinity and (c) sea surface temperature expressed as an average from 0 m to 75 m water depth. Data from the World Ocean Atlas 2005 [Antonov *et al.*, 2006; Locarnini *et al.*, 2006].

[31] Nitrate is essential for the growth and calcification of coccolithophores, and phosphate seems to act as a controlling agent of calcification [Baumann *et al.*, 2005]. Under present-day conditions, and focusing on the area surrounding ODP Site 1233, there are two likely sources for nutrients: the ACC, and the continental hinterland of Chile. The ACC is a typical high nutrient/low chlorophyll water mass, where use of the available nutrients such as nitrate or phosphate is limited by the low availability of micronutrients. Close to coastal areas, the availability of micronutrients increases mainly due to fluvial and airborne input, allowing very high productivity. The combination of macronutrients supplied by the ACC and the micronutrients washed into the ocean by high precipitation in this part of Chile results in high regional productivity [Hebbeln *et al.*, 2000].

[32] The absolute abundances of coccoliths (coccoliths/g) and the NAR (coccoliths $\text{cm}^{-2} \text{kyr}^{-1}$) at ODP Site 1233 follow the same trend, reaching higher values during the last glacial period than during Holocene times (see Figures 6k and 6l). Maximum values are recorded between ~19 and 22 kyr B.P., coinciding with the LGM ($\sim 3 \times 10^9$ coccoliths/g and NAR: $\sim 1.2 \times 10^{12}$ coccoliths $\text{cm}^{-2} \text{kyr}^{-1}$). The values decreased during the deglaciation, reaching minima between ~17–16.5 kyr B.P. and ~15.5–13.5 kyr B.P. Higher absolute

abundances of coccoliths and higher NAR values are seen again at around 16 kyr B.P. and from ~13 to 10 kyr B.P. ($\sim 2.5 \times 10^9$ coccoliths/g and $\sim 5 \times 10^{11}$ coccoliths $\text{cm}^{-2} \text{kyr}^{-1}$). The values are very low during the rest of the Holocene.

4.4. Diversity Index

[33] A Shannon index was calculated in order to evaluate the effect of the shifts of the oceanic fronts on coccolithophore diversity. For ODP Site 1233, this index varies between 1.05 (minimum reached at 18.6 kyr B.P.) and 2.04 (maximum at 15.4 kyr B.P.) for the last 27 kyr (Figure 6g). In general terms, a slight decreasing trend is seen from 27 kyr B.P. to 18.6 kyr B.P., together with a sudden increase from 18.6 kyr B.P. to 17.9 kyr B.P., followed by a less pronounced second increase from 17 kyr B.P. to 15.4 kyr B.P. A drop in diversity occurs from 15.3 kyr B.P. and to 13.3 kyr B.P., an increase from 13.3 kyr B.P. to 11.7 kyr B.P. and a decrease to the present.

5. Discussion

5.1. SST Reconstruction

[34] In general, our new SST record shares many features with the alkenone SST data set, in particular regarding the timing of the deglacial warming, the early Holocene

Figure 6. Comparison of coccolith derived SST records to other relevant records from 27 to 10 kyr B.P.: (a) three-point moving average SST reconstruction derived from the coccolithophore based temperature equation with a confidence interval stated at the 95% confidence level; (b) oxygen isotope ($\delta^{18}\text{O}\text{‰}$ SMOW) data from the Byrd ice core, Antarctica [Blunier and Brook, 2001]; (c) oxygen isotope ($\delta^{18}\text{O}\text{‰}$ SMOW) data from EPICA Dronning Maud Land ice core (EDML) drilled in Antarctica; (d) alkenone record from OPD Site 1233 [Lamy *et al.*, 2004, 2007]; (e) dinoflagellate species diversity calculated with the Shannon-Wiener diversity index [Verleye and Louwye, 2010]; (f) three-point moving average CEX' Index; (g) coccolithophore species diversity calculated with the Shannon diversity index; (h) first canonical variate from radiolarian multivariate data sets from ODP Site 1233 [Pisias *et al.*, 2006]; and (i) first canonical variate from pollen multivariate data sets from the same site [Pisias *et al.*, 2006]. Productivity related coccolith proxy data compared to the SST records from 27 to 0 kyr: (j) radiocarbon datings (^{14}C) marked with triangles (updated from Lamy *et al.* [2004, 2007]), (k) three-point moving average nannofossil accumulation rate (NAR) in coccoliths $\text{cm}^{-2} \text{kyr}^{-1}$, (l) three-point moving average coccoliths per gram of sediment, (m) NAR of *C. pelagicus* in coccoliths $\text{cm}^{-2} \text{kyr}^{-1}$, and (n) three-point moving average SST reconstruction derived from the coccolithophore based temperature equation with a confidence interval stated at the 95% confidence level. The gray bars indicate the Last Glacial Maximum (LGM), the Antarctic Cold Reversal (ACR), and the Holocene Climatic Optimum (HCO). In addition, the Younger Dryas (YD) cold period has been marked with a rectangle.

warming, and some millennial-scale fluctuations. The Last Glacial Maximum (LGM: 19–23 kyr B.P.) is not clearly defined, but the millennial-scale fluctuations observed in our SST reconstruction between 19 and 25 kyr B.P. broadly parallel the fluctuations in the alkenone SST record and Byrd ice core data (Figures 6b and 6d). Deglacial warming in our coccolithophore SST reconstruction starts after a final cold event at ~18.6 kyr B.P., with a SST of ~11.3°C. This is consistent with the alkenone SST obtained by *Lamy et al.* [2007], who documented the onset of deglaciation at 18.8 kyr B.P. and that reported by *Verleye and Louwye* [2010], who set it at 18.6 kyr B.P. using dinoflagellate cysts. The first deglacial warming phase also broadly coincides with the ice core records at Byrd located in the Pacific sector of Antarctica [*Blunier and Brook*, 2001] or Dronning Maud Land, EDML [*EPICA Community Members*, 2006] in the Atlantic sector, where deglacial warming began shortly after 18 kyr B.P. (Figures 6b and 6c).

[35] The maximum amplitude of reconstructed SST (the maximum SST minus minimum SST calculated) variations from ~27 kyr B.P. to 10 kyr B.P. is about 7.35°C, although the warming reconstructed over the last deglaciation is ~5°C, and hence slightly lower than the ~6–7°C revealed by the alkenone SST record. However, considering the intrinsic limitations of the method, the 95% lower limit of confidence interval traced for SST reconstruction (Figure 6a) suggests that the warming amplitude during deglaciation would be closer to 7°C.

[36] Because there is a correlation between SST and SSS (Figure 7), with a well marked latitudinal character (except for the Panama basin and in the southernmost offshore Chilean samples), factor 2 appears highly correlated with both variables (Table 2). Owing to the latitudinal pattern of this factor, we consider SST as the dominant oceanographic control parameter. Were this SSS, under present-day conditions we would have found higher values of factor 2 in low-salinity areas, such as the Panama basin, or would have noted the presence of few of the score species that characterize this factor in these regions.

5.2. LGM

[37] Our proxies indicate lower SSTs and higher NAR values during the LGM than today, interpreted in terms of higher coccolithophore productivity. The LGM assemblages are dominated by cold water species (e.g., *G. muelleriae* or *C. pelagicus*). *C. pelagicus* is the dominant species in the subarctic sector of the North Atlantic, but it is not found at high latitudes in the Southern Ocean [*Winter et al.*, 1999]. We confirmed the presence of the larger subspecies *C. pelagicus* spp. *braarudii*, although in low relative abundance (mean average of 1.2%, reaching maxima of 8.41%). This subspecies prefers temperate and cold waters and has been observed at low abundances in upwelling regimes [*Baumann et al.*, 2000; *Cachão and Moita*, 2000; *Geisen et al.*, 2002; *Parente et al.*, 2004]. Because *C. pelagicus* is not a species found at high abundances in the SH at high latitudes (e.g., close to the Subantarctic Zone [*Gravalosa et al.*, 2008]), our data suggest that the maximum NAR of this species during the LGM could have been linked to a high-fertility, cold, and

relatively mixed environment, in which high coccolithophore productivity occurred (Figure 6m). The radiolarian assemblages at Site 1233 [*Pisias et al.*, 2006] also support this conclusion (Figure 6h).

[38] Below we discuss two possible mechanisms for the enhanced glacial productivity at Site 1233:

[39] 1. One possible mechanism is an increase in the supply of macronutrients (such as nitrate or phosphate) due to an equatorward displacement of the northern margin of the ACC. This northward displacement or extension of the oceanographic system has been suggested previously in a number of studies and has been related to an equatorward shift of the Westerlies concomitant with a northward expansion of Antarctic sea ice [e.g., *Kim et al.*, 2002; *Lamy et al.*, 2004; *Mohtadi and Hebbeln*, 2004; *Kaiser et al.*, 2005], which would have influenced the whole oceanographic system along the Chilean slope and, likewise, continental paleoclimates. *Verleye and Louwye* [2010] suggested a ~7–10° northward shift of the system and even positioned the LGM Polar Front Zone (PFZ) at the latitude of ODP Site 1233. Our results point to a much more limited northward displacement. Classically it has often been considered that coccolithophore diversity decreases toward the South and becomes *E. huxleyi*-monospecific in Antarctic waters south of the Polar Front [*McIntyre and Bé*, 1967; *Gravalosa et al.*, 2008], suggesting a positive relationship of coccolithophore species diversity with SST and a negative relationship of the CEX' index with SST (Figure 6f). Therefore, SST changes offshore SE Chile can also be inferred from the Shannon index and CEX' values. If the PFZ had affected the study area during the LGM, the Shannon index values should have been closer to 0, indicating low diversity recorded at our site for this period of time. However, the Shannon indices (Figure 6g) are higher and indicate coccolithophore diversity values of 1.4, except for a marked drop at the onset of the deglaciation, suggesting that the PFZ remained south of our ODP Site 1233. A more limited northward movement of the Southern Ocean Fronts is consistent with a relatively small LGM sea ice expansion in the Pacific sector of the Southern Ocean [*Gersonde et al.*, 2005].

[40] 2. A higher micronutrient input (essentially iron) would have also contributed to stimulating marine productivity during the LGM. Owing to the significant expansion of the Patagonian Ice Sheet (PIS), reaching the island of Chiloé (41° 40'S at LGM and 45° 45'S today), glacial erosion processes would have strongly enhanced the glaciofluvial sediment flux from Fe-rich basaltic volcanics in the Andes [*Lamy et al.*, 2004]. Nevertheless, coccolithophores are better able to utilize Fe at low concentrations [*Martin et al.*, 1989; *Gregg and Casey*, 2007] and iron fertilization would have merely affected the large-celled phytoplankton: specifically diatoms [e.g., *Kolber et al.*, 1994; *Martin et al.*, 1994; *Harrison et al.*, 1999]. Therefore, we suggest that iron input did not play a major role in coccolithophore productivity enhancement, in close agreement with *Kaiser* [2005], who observed that alkenone production was not directly influenced by the iron concentrations at the same site.

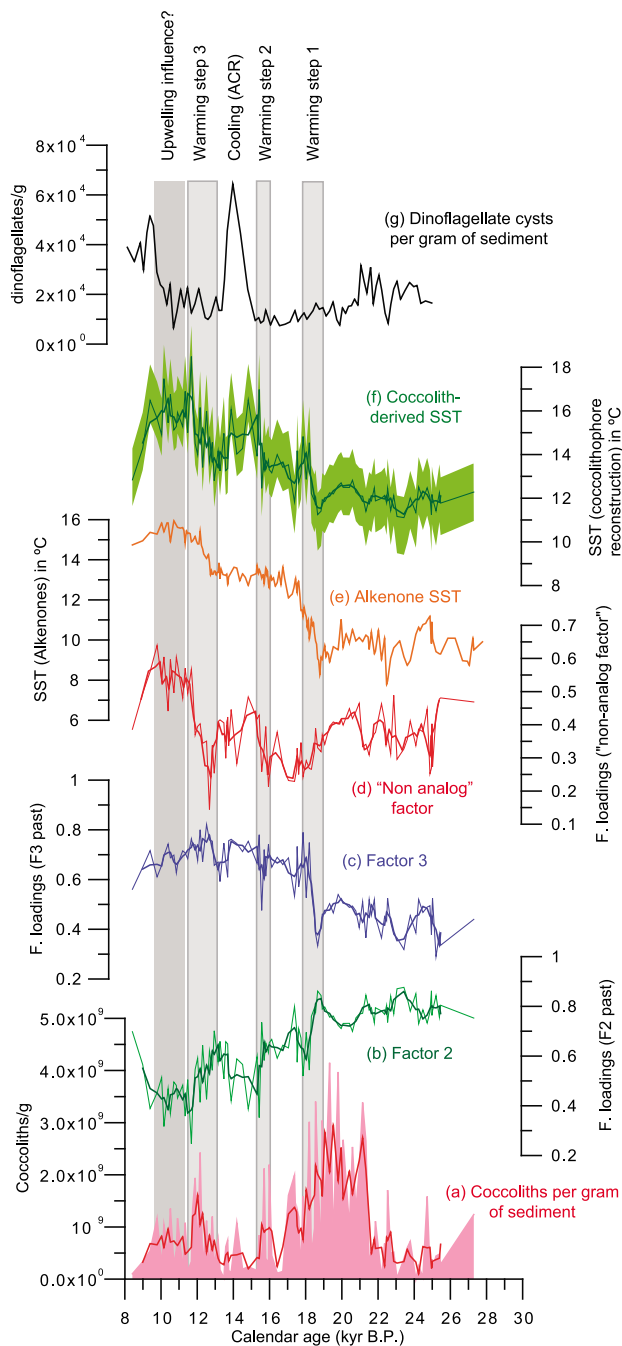


Figure 8. Records from 27 to 8 kyr at ODP Site 1233: (a) three-point moving average coccoliths per gram of sediment, (b) three-point moving average factor 2 loadings, (c) three-point moving average factor 3 loadings, (d) three-point moving average “nonanalog” loadings, (e) SST estimates derived from alkenones [Lamy *et al.*, 2004, 2007], (f) three-point moving average SST reconstruction derived from the coccolithophore based temperature equation with a confidence interval stated at the 95% confidence level, and (g) dinoflagellate cysts per gram of sediment [Verleye and Louwye, 2010]. The light gray bars indicate three major warming steps, and the dark gray bar indicates weak coastal upwelling conditions suggested in this work.

[41] Our results are consistent with previous paleoproductivity estimates off Chile [e.g., Mohtadi and Hebbeln, 2004] suggesting an increase in the advection of cold water and nutrients in the ACC/PCC, which might even have reached subtropical latitudes [Feldberg and Mix, 2002, 2003; Martínez *et al.*, 2003; Mohtadi and Hebbeln, 2004].

5.3. Deglaciation

[42] Our SST record shows that after the start of deglaciation (at ~18.6 kyr B.P.), three major warming steps are registered: from 18.6 to 18 kyr B.P.; 15.7 to 15.3 kyr B.P., and from 13 to 11.4 kyr B.P., broadly coinciding with increments in species diversity (Figures 6 and 8). These SST steps suggest that deglaciation is not recorded as a gradual continuous warming in South America, as stated by some authors [e.g., Ashworth and Hoganson, 1993]. The first and third warming steps are similar to the alkenone SST warmings.

[43] The first major step (18.6 to 18 kyr B.P.) would be characterized by a SST increase of ~2.6°C (although the maximum SST minus minimum SST calculated for this time interval is 3.3°C), also coinciding with a decrease in the NAR, caused by a slight drop in the availability of nutrients, as shown by an increase of factor 3 loadings (Figure 4) due to the anticorrelation of this factor with phosphate and nitrate. This rise in factor 3 loadings can be also linked to higher SSS, in agreement with Lamy *et al.* [2004].

[44] The second major step (15.7–15.3 kyr B.P.) would correspond to a warming period of ~2.5°C (although the maximum SST minus minimum SST calculated for this time interval is 4.5°C). The difference with the alkenone SSTs could be due to changes in the coccolithophore assemblage. During this period, the relative abundance of *E. huxleyi*, *G. oceanica* and *C. leptopus* increased while “small” *Gephyrocapsa* decreased. This is coincident with the sudden increase in the NAR, a slight decrease in the loadings of factor 3 (Figure 4) and an increase in the loadings of the “nonanalog” factor.

[45] The cooling (of ~2.4°C, although the maximum SST minus minimum SST calculated for this time interval is 3.3°C) that followed the second warming step (between 15.3 and 13 kyr B.P.) is not seen from the alkenone record, in which the two warming steps are separated by a “plateau” [Lamy *et al.*, 2007] (Figure 6d). The cooling broadly coincides with the Antarctic Cold Reversal (ACR: 14–12.5 kyr B.P.) [Jouzel *et al.*, 1995] found in other SH proxy records. Some examples include the oxygen isotope record ($\delta^{18}\text{O}$) from the Byrd ice core in Antarctica [Blunier and Brook, 2001] or the SST estimates derived from radiolarians (specifically, the first canonical variate extracted from the radiolarian record at ODP Site 1233) [Pisias *et al.*, 2006], in phase with respect to marine pollen assemblages (first canonical variate extracted from the pollen record at ODP Site 1233) [Pisias *et al.*, 2006]. As in the alkenone SST record from ODP Site 1233, the ACR cooling does not appear in the EDML $\delta^{18}\text{O}$ record [EPICA Community Members, 2006]. Even though an apparent cooling phase during this period coincident with a decrease in species diversity and an increase in the CEX’ index can be seen (Figure 6f), other authors [e.g., Markgraf *et al.*, 2007; Verleye

and Louwye, 2010] have interpreted it as an unstable period of intense seasonality. These differences regarding the ACR indicate that this event is not as clearly documented as the millennial fluctuations during MIS 3, and indeed the ACR appears to vary among proxy records and locations (Figure 6).

[46] In general, our results indicate a decrease in coccolithophore productivity from the LGM to the Holocene. We relate the changes in the NAR and in floral assemblages to variations in the dynamics of the surface water masses offshore Chile and to the two main potential sources of macronutrients and micronutrients: the ACC in first place and the PIS to a lesser extent. The decreasing trend of the NAR during deglaciation can be linked to the freshwater input from PIS melting and the subsequent stratification of the upper water column. The drop in nutrient content indicated by the predominance of factor 3 can be related to a reduction in the influence of the ACC and a general poleward displacement of the whole system.

[47] We consider a temporary return to glacial conditions during the climate reversal, when colder temperatures and an increasing trend of absolute abundances are recorded, probably linked to a slight northward movement of the atmospheric and oceanic systems, in agreement with *Pisias et al.* [2006]. The sudden higher availability of phosphate and nitrate would have been associated with the ACC nutrient supply.

[48] The change from high coccolithophore productivity during the LGM to lower productivity in the Holocene has also been recorded in other cores such as GeoB-3302 (32°S) offshore Chile with planktonic foraminifera [*Mohtadi and Hebbeln*, 2004]. However, SST patterns off central-south Chile reveal that warming during deglaciation was not uniform regionally and they imply different local responses [*Mohtadi et al.*, 2008].

5.4. Toward the Holocene

[49] Our record shows a third warming step of $\sim 3.4^{\circ}\text{C}$ (although the maximum SST minus minimum SST calculated for this time interval is 5.7°C) from ~ 13 to 11.4 kyr B.P., just after the ACR. This interval is also characterized by an increase in the NAR and in the “nonanalog” factor loadings, which point to a higher availability of nutrients and to the presence of more fertile waters. This time interval corresponds to the Northern Hemisphere Younger Dryas (YD: 13–11.5 kyr B.P.) suggesting a warming during this NH cold phase, as also observed in the alkenone record. The following warm interval from ~ 11.5 to the top of our high-resolution coccolith-derived SST record most likely represents the early part of the HCO in the region, as suggested by the alkenone SST record [*Kaiser et al.*, 2005]. The nanofloral SST reaches 18.5°C , but this value is overestimated since factor 2 is not appropriate for the reconstruction of warmer temperatures (see residuals in Figure 5). A more realistic value is indicated by the SST three-point moving average indicated in Figures 6 and 8 of $\sim 16.8^{\circ}\text{C}$.

[50] During the HCO a general lowering in the NAR occurred, except for a slight increase from ~ 9.5 kyr B.P. to ~ 11.5 kyr B.P. in the NAR and in the “nonanalog” factor loadings. The inferred reduction in the nutrient supply would

mainly correspond to the maximum poleward shift of the atmospheric and oceanic systems.

[51] Locally, weak coastal upwelling conditions would have influenced the coccolithophore assemblages in the early HCO, as suggested by the increase in *G. oceanica*, a species typically found in fertile water conditions [*Giraudeau and Bailey*, 1995], and also in the “nonanalog” factor loadings, coincident with the slight drop in factor 3 loadings (Figure 4). We propose a temporary enrichment in nutrients when the ACC reached its southernmost position for the time frame studied. This is in agreement with *Verleye and Louwye* [2010], who recorded the lowest concentrations of dinoflagellate cysts (see Figure 8g) for the HCO and an increase in the abundance of upwelling-related species and cysts.

6. Conclusions

[52] Nanofloral high-resolution SST estimates show good concordance with alkenone SST values for the last deglaciation [*Lamy et al.*, 2004, 2007] obtained at ODP Site 1233 (41°S off southern Chile). This promising method has a great potential for the reconstruction of accurate paleotemperatures, comparable to those obtained using independent proxies (e.g., alkenone-based SSTs). However, further refinements (i.e., development of more sophisticated statistical models, dealing with some of the nonlinearities ascertained in the presented calibrations) would be helpful for a better understanding of the minor discrepancies observed between independent proxies such as alkenone-derived SSTs and our nanofloral SST estimates.

[53] The Last Glacial Maximum (LGM: 19–23 kyr B.P.) is not clearly defined, but deglacial warming in our nanofloral SSTs reconstruction starts after a final cold event at ~ 18.6 kyr B.P., with a SST of $\sim 11.3^{\circ}\text{C}$. Our SST record shows that after the starting of deglaciation (at 18.6 kyr B.P.), three major warming steps are recorded: from 18.6 to 18 kyr B.P. ($\sim 2.6^{\circ}\text{C}$), 15.7 to 15.3 kyr ($\sim 2.5^{\circ}\text{C}$) B.P., and from 13 to 11.4 kyr B.P. ($\sim 3.4^{\circ}\text{C}$). Between 15.3 and 13 kyr B.P. a cooling of $\sim 2.4^{\circ}\text{C}$ is also recorded, coincident with the ACR, which has also been recorded by radiolarian and pollen records [*Pisias et al.*, 2006] at ODP Site 1233.

[54] Combining the SST reconstruction with absolute coccolith abundances and accumulation rates, we show that the colder temperatures during the LGM are linked to higher coccolithophore productivity offshore Chile and to a northward displacement of the Southern Westerlies and the ACC. During the HCO, warmer SSTs and lower coccolithophore productivity with indications of weak coastal upwelling suggest a poleward shift of the whole system, i.e., to a more southward location than today.

Appendix A: Taxonomic Appendix

[55] *Braarudosphaera bigelowii* (Gran and Braarud, 1935) Deflandre 1947

[56] *Calcidiscus leptoporus* (Murray and Blackman, 1898) Loeblich and Tappan, 1978

[57] *Calciosolenia* Gran, 1912, emend. Young et al., 2003

[58] *Coccolithus pelagicus* (Wallich, 1877) Schiller, 1930

- [59] *Coccolithus pelagicus* ssp. *braarudii* (Gaarder, 1962) Geisen et al., 2000
- [60] *Emiliania huxleyi* (Lohmann, 1902) Hay and Mohler in Hay et al., 1967
- [61] *Florisphaera profunda* Okada and Honjo, 1973
- [62] *Gephyrocapsa* Kamptner, 1943
- [63] *Gephyrocapsa ericsonii* [McIntyre and Bé, 1967] (grouped in “small” *Gephyrocapsa*, *Gephyrocapsa* coccolith <3 μm long)
- [64] *Gephyrocapsa muelleriae* Br  h  ret, 1978
- [65] *Gephyrocapsa oceanica* Kamptner, 1943
- [66] *Helicosphaera* Kamptner, 1954
- [67] *Helicosphaera carteri* (Wallich, 1877) Kamptner, 1954
- [68] *Oolithotus* Reinhardt in Cohen and Reinhardt, 1968
- [69] *Rhabdosphaera clavigera* Murray and Blackman, 1898
- [70] *Umbellosphaera* Paasche in Markali and Paasche, 1955
- [71] *Umbilicosphaera* Lohmann, 1902
- [72] **Acknowledgments.** The reviewers are acknowledged for their critical evaluation, constructive opinions, and helpful suggestions. The authors wish to thank O. Romero, A. Mix, F. Abrantes, D. Hebbeln, and M. Mohtadi for the material supplied. Karl-Heinz Baumann and Babette Boeckel are thanked for their suggestions. N. Pisi  s is thanked for providing data. This work was funded by the Spanish “Ministerio de Ciencia e Innovaci  n” MICINN project PASUR CGL2009-08651 and GRACCIE (CONSO-LIDER-INGENIO CSD 2007-00067), the Regional government of Castilla and Leon project GR34Project, and a MEC FPU grant (AP-2004-2374) awarded to Mariem Saavedra-Pellitero.

References

- Abrantes, F., C. Lopes, A. Mix, and N. Pisi  s (2007), Diatoms in southeast Pacific surface sediments reflect environmental properties, *Quat. Sci. Rev.*, 26(1–2), 155–169, doi:10.1016/j.quascirev.2006.02.022.
- Antonov, J. I., R. A. Locarnini, T. P. Boyer, A. V. Mishonov, and H. E. Garcia (2006), *World Ocean Atlas 2005*, vol. 2, *Salinity*, NOAA Atlas NESDIS, vol. 62, edited by S. Levitus, 182 pp., U.S. Gov. Print. Off., Washington, D. C.
- Ashworth, A. C., and J. W. Hoganson (1993), The magnitude and rapidity of the climate change marking the end of the Pleistocene in the mid-latitudes of South America, *Palaeogeogr. Palaeoclimatol. Palaeoecol.*, 101(3–4), 263–270, doi:10.1016/0031-0182(93)90018-E.
- Blackman, J., and N. J. Shackleton (1983), Quantitative biochronology of Pliocene and early Pleistocene calcareous nannofossils from the Atlantic, Indian and Pacific oceans, *Mar. Micropaleontol.*, 8(2), 141–170, doi:10.1016/0377-8398(83)90009-9.
- Baumann, K.-H., H. Andr  uleit, and C. Santsleben (2000), Coccolithophores in the Nordic seas: Comparison of living communities with surface sediment assemblages, *Deep Sea Res., Part II*, 47(9–11), 1743–1772, doi:10.1016/S0967-0645(00)00005-9.
- Baumann, K.-H., B. B  ckel, and M. Frenz (2004), Coccolith contribution to South Atlantic carbonate sedimentation, in *Coccolithophores: From Molecular Processes to Global Impact*, edited by H. R. Thierstein and J. R. Young, pp. 367–402, Springer, Berlin.
- Baumann, K.-H., H. Andr  uleit, B. B  ckel, M. Geisen, and H. Kinkel (2005), The significance of extant coccolithophores as indicators of ocean water masses, surface water temperature, and palaeoproductivity: A review, *Palaeontol. Z.*, 79(1), 93–112, doi:10.1007/BF03021756.
- Berger, W. H., C. G. Adelseck Jr., and L. A. Mayer (1976), Distribution of carbonate in surface sediments of the Pacific Ocean, *J. Geophys. Res.*, 81, 2617–2627, doi:10.1029/JC081i015p02617.
- Berger, W. H., K. Fischer, C. Lai, and G. Wu (1987), Ocean productivity and organic flux, part I: Overview and maps of primary production and export production, *SIO Ref. Ser.*, 67, 87–130, Scripps Inst. of Oceanogr., San Diego, Calif.
- Billard, C., and I. Inouye (2004), What is new in coccolithophore biology?, in *Coccolithophores: From Molecular Processes to Global Impact*, edited by H. R. Thierstein and J. R. Young, pp. 1–30, Springer, Berlin.
- Blunier, T., and E. J. Brook (2001), Timing of millennial-scale climate change in Antarctica and Greenland during the Last Glacial Period, *Science*, 291(5501), 109–112, doi:10.1126/science.291.5501.109.
- Boeckel, B., and K. H. Baumann (2004), Distribution of coccoliths in surface sediments of the south-eastern South Atlantic Ocean: Ecology, preservation and carbonate contribution, *Mar. Micropaleontol.*, 51(3–4), 301–320, doi:10.1016/j.marmicro.2004.01.001.
- Brand, L. E. (1994), Physiological ecology of marine coccolithophores, in *Coccolithophores*, edited by A. Winter and W. G. Siesser, pp. 39–49, Cambridge Univ. Press, New York.
- Broecker, W. S., and S. Broecker (1974), Carbonate dissolution on the western flank of the East Pacific Rise, in *Studies in Paleo-Oceanography*, edited by W. W. Hay, *Spec. Publ. Soc. Econ. Paleontol. Mineral.*, 20, 44–57.
- Broerse, A. T. C., G. J. A. Brummer, and J. E. V. Hinte (2000), Coccolithophore export production in response to monsoonal upwelling off Somalia (northwestern Indian Ocean), *Deep Sea Res., Part II*, 47(9–11), 2179–2205, doi:10.1016/S0967-0645(00)00021-7.
- Brown, C. W., and J. A. Yoder (1994), Coccolithophorid blooms in the global ocean, *J. Geophys. Res.*, 99(C4), 7467–7482, doi:10.1029/93JC02156.
- Cach  o, M., and M. T. Moita (2000), *Coccolithus pelagicus*, a productivity proxy related to moderate fronts off western Iberia, *Mar. Micropaleontol.*, 39(1–4), 131–155, doi:10.1016/S0377-8398(00)00018-9.
- Cane, M. A. (1998), A role for the tropical Pacific, *Science*, 282(5386), 59–61, doi:10.1126/science.282.5386.59.
- Chapman, M. R., N. J. Shackleton, M. Zhao, and G. Eglinton (1996), Faunal and alkenone reconstructions of subtropical North Atlantic surface hydrography and paleotemperature over the last 28 kyr, *Paleoceanography*, 11(3), 343–357, doi:10.1029/96PA00041.
- Clement, A. C., R. Seager, and M. A. Cane (1999), Orbital controls on the El Ni  o/Southern Oscillation and the tropical climate, *Paleoceanography*, 14(4), 441–456, doi:10.1029/1999PA900013.
- D  vila, P. M., D. Figueroa, and E. M  ller (2002), Freshwater input into the coastal ocean and its relation with the salinity distribution off austral Chile (35–55  S), *Cont. Shelf Res.*, 22(3), 521–534, doi:10.1016/S0278-4343(01)00072-3.
- Deacon, G. E. R. (1933), A general account of the hydrology of the South Atlantic Ocean, *Discovery Rep.*, 7, 177–238.
- Dittert, N., K.-H. Baumann, T. Bickert, R. Henrich, R. Huber, H. Kinkel, and H. Meggers (1999), Carbonate dissolution in the deep sea: Methods, quantification and paleoceanographic application, in *Use of Proxies in Paleoceanography: Examples From the South Atlantic*, edited by G. Fischer and G. Wefer, pp. 255–284, Springer, Berlin.
- EPICA Community Members (2006), One-to-one coupling of glacial climate variability in Greenland and Antarctica, *Nature*, 444(7116), 195–198, doi:10.1038/nature05301.
- Farrell, J. W., and W. L. Prell (1989), Climatic change and CaCO₃ preservation: An 800,000 year bathymetric reconstruction from the central equatorial Pacific Ocean, *Paleoceanography*, 4, 447–466, doi:10.1029/PA004i004p00447.
- Fatela, F., and R. Taborda (2002), Confidence limits of species proportions in microfossil assemblages, *Mar. Micropaleontol.*, 45(2), 169–174, doi:10.1016/S0377-8398(02)00021-X.
- Feldberg, M. J., and A. C. Mix (2002), Sea-surface temperature estimates in the southeast Pacific based on planktonic foraminiferal species; modern calibration and Last Glacial Maximum, *Mar. Micropaleontol.*, 44, 1–29, doi:10.1016/S0377-8398(01)00035-4.
- Feldberg, M. J., and A. C. Mix (2003), Planktonic foraminifera, sea surface temperatures, and mechanisms of oceanic change in the Peru and south equatorial currents, 0–150 ka BP, *Paleoceanography*, 18(1), 1016, doi:10.1029/2001PA000740.
- Findlay, C. S., J. R. Young, and F. J. Scott (2005), Haptophytes: Order Coccolithophorales, in *Antarctic Marine Protists*, edited by F. J. Scott and H. J. Marchant, pp. 276–294, Aust. Biol. Resour. Study, Canberra, A. C. T., Australia.
- Flores, J. A., and F. J. Sierro (1997), Revised technique for calculation of calcareous nannofossil accumulation rates, *Micropaleontology*, 43, 321–324, doi:10.2307/1485832.
- Geisen, M., C. Billard, A. T. C. Broerse, L. Cros, I. Probert, and J. R. Young (2002), Life-cycle associations involving pairs of holococcolithophorid species: Intraspecific variation or cryptic speciation?, *Eur. J. Phycol.*, 37(4), 531–550, doi:10.1017/S09670262003852.
- Gersonde, R., X. Crosta, A. Abelmann, and L. Armand (2005), Sea-surface temperature and sea ice distribution of the Southern Ocean at the EPILOG Last Glacial Maximum—A

- circum-Antarctic view based on siliceous microfossil records, *Quat. Sci. Rev.*, *24*, 869–896, doi:10.1016/j.quascirev.2004.07.015.
- Giraudeau, J., and G. W. Bailey (1995), Spatial dynamics of coccolithophore communities during an upwelling event in the southern Benguela system, *Cont. Shelf Res.*, *15*(14), 1825–1852, doi:10.1016/0278-4343(94)00095-5.
- Giraudeau, J., G. W. Bailey, and C. Pujol (2000), A high-resolution time-series analyses of particle fluxes in the northern Benguela coastal upwelling system: Carbonate record of changes in biogenic production and particle transfer processes, *Deep Sea Res., Part II*, *47*(9–11), 1999–2028, doi:10.1016/S0967-0645(00)00014-X.
- Gravalosa, J. M., J.-A. Flores, F. J. Sierro, and R. Gersonde (2008), Sea surface distribution of coccolithophores in the eastern Pacific sector of the Southern Ocean (Bellingshausen and Amundsen seas) during the late austral summer of 2001, *Mar. Micropaleontol.*, *69*(1), 16–25, doi:10.1016/j.marmicro.2007.11.006.
- Gregg, W. W., and N. W. Casey (2007), Modeling coccolithophores in the global oceans, *Deep Sea Res., Part II*, *54*(5–7), 447–477, doi:10.1016/j.dsr2.2006.12.007.
- Harrison, P. J., P. W. Boyd, D. E. Varela, S. Takeda, A. Shiimoto, and T. Odate (1999), Comparison of factors controlling phytoplankton productivity in the NE and NW subarctic Pacific gyres, *Prog. Oceanogr.*, *43*, 205–234, doi:10.1016/S0079-6611(99)00015-4.
- Hebbeln, D., M. Marchant, T. Freudenthal, and G. Wefer (2000), Surface sediment distribution along the Chilean continental slope related to upwelling and productivity, *Mar. Geol.*, *164*(3–4), 119–137, doi:10.1016/S0025-3227(99)00129-2.
- Iriarte, J. L., H. E. González, K. K. Liu, C. Rivas, and C. Valenzuela (2007), Spatial and temporal variability of chlorophyll and primary productivity in surface waters of southern Chile (41.5–43° S), *Estuarine Coastal Shelf Sci.*, *74*, 471–480, doi:10.1016/j.ecss.2007.05.015.
- Jouzel, J., et al. (1995), The two-step shape and timing of the last deglaciation in Antarctica, *Clim. Dyn.*, *11*(3), 151–161, doi:10.1007/BF00223498.
- Kaiser, J. (2005), Sea-surface temperature variability in the southeast Pacific during the last glacial-interglacial cycle and relationships to paleoenvironmental changes in central and southern Chile, Ph.D. thesis, DFG-Res. Cent. Ocean Margins, Univ. Bremen, Bremen, Germany.
- Kaiser, J., F. Lamy, and D. Hebbeln (2005), A 70-kyr sea surface temperature record off southern Chile (Ocean Drilling Program Site 1233), *Paleoceanography*, *20*, PA4009, doi:10.1029/2005PA001146.
- Kaiser, J., F. Lamy, H. W. Arz, and D. Hebbeln (2007), Dynamics of the millennial-scale sea surface temperature and Patagonian Ice Sheet fluctuations in southern Chile during the last 70 kyr (ODP Site 1233), *Quat. Int.*, *161*(1), 77–89, doi:10.1016/j.quaint.2006.10.024.
- Kim, J.-H., R. R. Schneider, D. Hebbeln, P. J. Müller, and G. Wefer (2002), Last deglacial sea-surface temperature evolution in the southeast Pacific compared to climate changes on the South American continent, *Quat. Sci. Rev.*, *21*(18–19), 2085–2097, doi:10.1016/S0277-3791(02)00012-4.
- Kleijne, A., D. Kroon, and W. Zevenboom (1989), Phytoplankton and foraminiferal frequencies in northern Indian Ocean and Red Sea surface waters, *Neth. J. Sea Res.*, *24*, 531–539, doi:10.1016/0077-7579(89)90131-2.
- Kolber, Z. S., R. T. Barber, K. H. Coale, S. E. Fitzwater, R. M. Greene, K. S. Johnson, S. Lindley, and P. G. Falkowski (1994), Iron limitation of phytoplankton photosynthesis in the equatorial Pacific Ocean, *Nature*, *371*, 145–149, doi:10.1038/371145a0.
- Koutavas, A., and J. P. Sachs (2008), Northern timing of deglaciation in the eastern equatorial Pacific from alkenone paleothermometry, *Paleoceanography*, *23*, PA4205, doi:10.1029/2008PA001593.
- Kucera, M., A. Rosell-Melé, R. Schneider, C. Waelbroeck, and M. Weinelt (2005a), Multiproxy approach for the reconstruction of the glacial ocean surface (MARGO), *Quat. Sci. Rev.*, *24*(7–9), 813–819, doi:10.1016/j.quascirev.2004.07.017.
- Kucera, M., et al. (2005b), Reconstruction of sea-surface temperatures from assemblages of planktonic foraminifera: Multi-technique approach based on geographically constrained calibration data sets and its application to glacial Atlantic and Pacific oceans, *Quat. Sci. Rev.*, *24*(7–9), 951–998, doi:10.1016/j.quascirev.2004.07.014.
- Lamy, F., and J. Kaiser (2009), Glacial to Holocene paleoceanographic and continental paleoclimate reconstructions based on ODP Site 1233/GeoB 3313 off southern Chile, in *Past Climate Variability in South America and Surrounding Regions: From the Last Glacial Maximum to the Holocene*, vol. 14, edited by F. Vimeux, pp. 129–156, Springer, Berlin.
- Lamy, F., D. Hebbeln, and G. Wefer (1998), Terrigenous sediment supply along the Chilean continental margin: Modern regional patterns of texture and composition, *Geol. Rundsch.*, *87*(3), 477–494, doi:10.1007/s005310050223.
- Lamy, F., D. Hebbeln, U. Röhl, and G. Wefer (2001), Holocene rainfall variability in southern Chile: A marine record of latitudinal shifts of the southern westerlies, *Earth Planet. Sci. Lett.*, *185*(3–4), 369–382, doi:10.1016/S0012-821X(00)00381-2.
- Lamy, F., J. Kaiser, U. Ninnemann, D. Hebbeln, H. W. Arz, and J. Stoner (2004), Antarctic timing of surface water changes off Chile and Patagonian Ice Sheet response, *Science*, *304*, 1959–1962, doi:10.1126/science.1097863.
- Lamy, F., J. Kaiser, H. W. Arz, D. Hebbeln, U. Ninnemann, O. Timm, A. Timmermann, and J. R. Toggweiler (2007), Modulation of the bipolar seesaw in the southeast Pacific during Termination 1, *Earth Planet. Sci. Lett.*, *259*(3–4), 400–413, doi:10.1016/j.epsl.2007.04.040.
- Lea, D. W. (2003), Elemental and isotopic proxies of past ocean temperatures, in *Treatise on Geochemistry*, vol. 6, *The Oceans and Marine Geochemistry*, edited by H. Elderfield, pp. 365–390, Elsevier, Amsterdam.
- Leduc, G., R. Schneider, J.-H. Kim, and G. Lohmann (2010), Holocene and Eemian sea surface temperature trends as revealed by alkenone and Mg/Ca paleothermometry, *Quat. Sci. Rev.*, *29*, 989–1004, doi:10.1016/j.quascirev.2010.01.004.
- Locarnini, R. A., A. V. Mishonov, J. I. Antonov, T. P. Boyer, and H. E. Garcia (2006), *World Ocean Atlas 2005*, vol. 1, *Temperature*, NOAA Atlas NESDIS, vol. 61, edited by S. Levitus, 182 pp., U.S. Gov. Print. Off., Washington, D. C.
- López-Otálvaro, G.-E., J. A. Flores, F. J. Sierro, I. Cacho, J.-O. Grimalt, E. Michel, E. Cortijo, and L. Labeyrie (2009), Late Pleistocene paleoproductivity patterns during the last climatic cycle in the Guyana Basin as revealed by calcareous nannoplankton, *eEarth*, *4*, 1–13.
- Markgraf, V., C. Whitlock, and S. Haberle (2007), Vegetation and fire history during the last 18,000 cal yr B.P. in the Southern Patagonia: Mallín Pollux, Coyhaique, Province Aisén (45°41'30"S, 71°50'30"W, 640 m elevation), *Paleogeogr. Palaeoclimatol. Palaeoecol.*, *254*, 492–507, doi:10.1016/j.palaeo.2007.07.008.
- Marlowe, I. T., S. C. Brassell, G. Eglinton, and J. C. Green (1990), Long-chain alkenones and alkyl alkenoates and the fossil coccolith record of marine sediments, *Chem. Geol.*, *88*(3–4), 349–375, doi:10.1016/0009-2541(90)90098-R.
- Martin, J. H., R. M. Gordon, S. Fitzwater, and W. W. Broenkow (1989), Vertex: Phytoplankton/iron studies in the Gulf of Alaska, *Deep Sea Res.*, *36*(5), 649–680, doi:10.1016/0198-0149(89)90144-1.
- Martin, J. H., K. H. Coale, and K. S. Johnson (1994), Testing the iron hypothesis in ecosystems of the equatorial Pacific Ocean, *Nature*, *371*, 123–129, doi:10.1038/371123a0.
- Martínez, I., L. Keigwin, T. T. Barrows, Y. Yokoyama, and J. Southon (2003), La Niña-like conditions in the eastern equatorial Pacific and a stronger Choco jet in the northern Andes during the last glaciation, *Paleoceanography*, *18*(2), 1033, doi:10.1029/2002PA000877.
- McIntyre, A., and A. W. H. Bé (1967), Modern coccolithophoridae of the Atlantic Ocean—Placoliths and cyrtoliths, *Deep Sea Res.*, *14*, 561–597.
- McPhaden, M. J., S. E. Zebiak, and H. Glantz (2006), ENSO as an integrating concept in Earth science, *Science*, *314*(5806), 1740–1745, doi:10.1126/science.1132588.
- Miller, A. (1976), The climate of Chile, in *Climates of Central and South America*, edited by W. E. Schwerdtfeger, pp. 113–145, Elsevier, Amsterdam.
- Mitchell-Innes, B. A., and A. Winter (1987), Coccolithophores: A major phytoplankton component in mature upwelled waters off the Cape Peninsula, South Africa in March, 1983, *Mar. Biol. Berlin*, *95*(1), 25–30, doi:10.1007/BF00447481.
- Mix, A. C. (2006), Running hot and cold in the eastern equatorial Pacific, *Quat. Sci. Rev.*, *25*, 1147–1149, doi:10.1016/j.quascirev.2006.03.008.
- Mix, A. C., A. E. Morey, N. G. Pisias, and S. W. Hostetler (1999), Foraminiferal faunal estimates of paleotemperature: Circumventing the no-analog problem yields cool ice age tropics, *Paleoceanography*, *14*(3), 350–359, doi:10.1029/1999PA900012.
- Mix, A. C., R. Tiedemann, P. Blum, and Shipboard Scientists (2003), *Leg 202 Summary*, 145 pp., Ocean Drill. Program, College Station, Tex.
- Mohtadi, M., and D. Hebbeln (2004), Mechanisms and variations of the paleoproductivity off northern Chile (24°S–33°S) during the last 40,000 years, *Paleoceanography*, *19*, PA2023, doi:10.1029/2004PA001003.
- Mohtadi, M., P. Rossel, C. B. Lange, S. Pantoja, P. Böning, D. J. Repeta, M. Grunwald, F. Lamy, D. Hebbeln, and H.-J. Brumsack (2008), Deglacial pattern of circulation and marine productivity in the upwelling region off central-south Chile, *Earth Planet. Sci.*

- Lett.*, 272(1–2), 221–230, doi:10.1016/j.epsl.2008.04.043.
- Morey, A. E., A. C. Mix, and N. G. Pisias (2005), Planktonic foraminiferal assemblages preserved in surface sediments correspond to multiple environment variables, *Quat. Sci. Rev.*, 24(7–9), 925, doi:10.1016/j.quascirev.2003.09.011.
- Orsi, A. H., T. Whitworth III, and W. D. Nowlin Jr. (1995), On the meridional extent and fronts of the Antarctic Circumpolar Current, *Deep Sea Res.*, 42, 641–673, doi:10.1016/0967-0637(95)00021-W.
- Parente, A., M. Cachao, K. H. Baumann, L. de Abreu, and J. Ferreira (2004), Morphometry of *Coccolithus pelagicus* s.l. (Coccolithophore, Haptophyta) from offshore Portugal, during the last 200 kyr, *Micropaleontology*, 50(1), 107–120, doi:10.2113/50.Suppl_1.107.
- Pienaar, R. N. (1994), Ultrastructure and calcification of coccolithophores, in *Coccolithophores*, edited by E. A. Winter and W. G. Siesser, pp. 13–39, Cambridge Univ. Press, Cambridge, U. K.
- Pisias, N. G., A. Roelofs, and M. Weber (1997), Radiolarian-based transfer functions for estimating mean surface ocean temperatures and seasonal range, *Paleoceanography*, 12, 365–379, doi:10.1029/97PA00582.
- Pisias, N. G., L. Heusser, C. Heusser, S. W. Hostetler, A. C. Mix, and M. Weber (2006), Radiolaria and pollen records from 0 to 50 ka at ODP Site 1233: Continental and marine climate records from the southeast Pacific, *Quat. Sci. Rev.*, 25(5–6), 455–473, doi:10.1016/j.quascirev.2005.06.009.
- Prahl, F. G., and S. G. Wakeham (1987), Calibration of unsaturation patterns in long-chain ketone compositions for palaeotemperature assessment, *Nature*, 330(6146), 367–369, doi:10.1038/330367a0.
- Saavedra-Pellitero, M., J. A. Flores, K. H. Baumann, and F. J. Sierro (2010), Coccolith distribution patterns in surface sediments of equatorial and southeastern Pacific Ocean, *Geobios*, 43, 131–149, doi:10.1016/j.geobios.2009.09.004.
- Shaffer, G., S. Salinas, O. Pizarro, A. Vega, and S. Hormazabal (1995), Currents in the deep ocean off Chile (30°S), *Deep Sea Res., Part I*, 42(4), 425–436, doi:10.1016/0967-0637(95)99823-6.
- Steinke, S., M. Kienast, J. Groeneveld, L.-C. Lin, M.-T. Chen, and R. Rendle-Bühring (2008), Proxy dependence of the temporal pattern of deglacial warming in the tropical South China Sea: Toward resolving seasonality, *Quat. Sci. Rev.*, 27, 688–700, doi:10.1016/j.quascirev.2007.12.003.
- Steinmetz, J. C. (1994), Sedimentation of coccolithophores, in *Coccolithophores*, edited by A. Winter and W. G. Siesser, pp. 179–197, Cambridge Univ. Press, Cambridge, U. K.
- Streten, N. A., and J. W. Zillmann (1984), Climate of the South Pacific Ocean, in *Climate of the Oceans*, vol. 15, edited by H. van Loon, pp. 263–429, Elsevier, Amsterdam.
- Strub, P. T., J. M. Mesias, V. Montecino, J. Ruttlant, and S. Salinas (1998), Coastal ocean circulation off western South America, in *The Sea: Global Coastal Ocean*, vol. 11, edited by A. R. Robinson and K. H. Brink, pp. 273–313, John Wiley, New York.
- Thompson, P. R. (1976), Planktonic foraminiferal dissolution and the progress towards a Pleistocene equatorial Pacific transfer function, *J. Foraminiferal Res.*, 6, 208–227, doi:10.2113/gsjfr.6.3.208.
- Verleye, T. J., and S. Louwye (2010), Late Quaternary environmental changes and latitudinal shifts of the Antarctic Circumpolar Current as recorded by dinoflagellate cysts from offshore Chile (41°S), *Quat. Sci. Rev.*, 29, 1025–1039, doi:10.1016/j.quascirev.2010.01.009.
- Volkman, J. K., G. Eglinton, E. D. S. Corner, and T. E. V. Forsberg (1980), Long-chain alkenes and alkenones in the marine coccolithophorid *Emiliania huxleyi*, *Phytochemistry*, 19(12), 2619–2622, doi:10.1016/S0031-9422(00)83930-8.
- Wefer, G., W. H. Berger, J. Bijma, and G. Fischer (1999), Clues to ocean history: A brief overview of proxies, in *Use of Proxies in Paleoceanography: Examples From the South Atlantic*, edited by G. Fischer and G. Wefer, pp. 1–68, Springer, Berlin.
- Winter, A., R. W. Jordan, and P. H. Roth (1994), Biogeography of living coccolithophores in ocean waters, in *Coccolithophores*, edited by A. Winter and W. G. Siesser, pp. 161–178, Cambridge Univ. Press, Cambridge, U. K.
- Winter, A., M. Elbrächter, and G. Krause (1999), Subtropical coccolithophores in the Weddell Sea, *Deep Sea Res., Part I*, 46(3), 439–449, doi:10.1016/S0967-0637(98)00076-4.
- Wyrтки, K. (1981), An estimate of equatorial upwelling in the Pacific, *J. Phys. Oceanogr.*, 11(9), 1205–1214, doi:10.1175/1520-0485(1981)011<1205:AEOEUI>2.0.CO;2.
- Young, J. R. (1994), Functions of coccoliths, in *Coccolithophores*, edited by A. Winter and W. G. Siesser, pp. 63–82, Cambridge Univ. Press, Cambridge, U. K.

A. Cortina, J. A. Flores, M. Saavedra-Pellitero, and F. J. Sierro, Department of Geology, University of Salamanca, Plaza de la Merced s/n, E-37008 Salamanca, Spain. (mariemsaavedra@usal.es)

F. Lamy, Alfred Wegener Institute for Polar and Marine Research, Am Alten Hafen 26, D-27568 Bremerhaven, Germany.